complexes of well-defined geometry, an alternative method for introducing stereochemical information into the refinement of an unknown system such as a metalloprotein is to treat the stereochemical conditions of fixed imidazole geometry as additional observations. This approach has been used in the least-squares refinement of Hendrickson and Konnert[29] for the crystallographic determination of protein structure, where a similar problem of underdeterminancy exists; i.e., the ratio of the number of observations to parameters is typically not more than two. We believe that such an approach combined with the multiple-scattering formalism will allow a more detailed and less ambiguous treatment, as well as offer the potential for extracting information relating to the degree of asymmetry of histidine coordination in metalloproteins.

Acknowledgment. We thank the Daresbury Laboratory for use of facilities. The work was carried out under a S.E.R.C. grant to N.J.B., P.F.K., and S.S.H. S.S.H. thanks Professor Charles E. Bugg (Director, Centre for Macromolecular Crystallography, University of Alabama at Birmingham) for his hospitality during a sabbatical stay.

(29) Hendrickson, W. A.; Konnert, J. H. *Proc. Madras Symp. Biomol. Struct. Conform. Function Evol.* **1981**, 43-57.
(30) Boland, J. J.; Crane, S. E.; Baldeschwieler, J. D. *J. Chem. Phys.* **1982**, *77*, 142-153.

Anion Binding to Bovine Erythrocyte Superoxide Dismutase Studied by X-ray Absorption Spectroscopy. A Detailed Structural Analysis of the Native Enzyme and the Azido and Cyano Derivatives Using a Multiple-Scattering Approach

Ninian J. Blackburn,*[1a] Richard W. Strange,[1a] Loretta M. McFadden,[1a] and S. Samar Hasnain[1b]

Contribution from the Department of Chemistry, University of Manchester Institute of Science and Technology, Manchester, M60 1QD, United Kingdom, and S.E.R.C. Daresbury Laboratory, Warrington, Cheshire, WA4 4AD, United Kingdom. *Received January 30, 1987*

Abstract: X-ray absorption spectra are reported for the native, azide-bound, and cyanide-bound forms of bovine erythrocyte superoxide dismutase (SOD). Absorption edge data suggest a similar geometric structure for the native enzyme and the azido derivative, but a different coordination structure for the cyano derivative. Analysis of the EXAFS, using a recently developed multiple-scattering method for treating systems containing metal–histidine coordination, has allowed accurate simulation of the raw unfiltered EXAFS data over the range $k = 3$–13 Å^{-1}. The analysis has provided structural details of the coordinated imidazole rings in addition to structural parameters for the coordinated anions. Thus azide is coordinated in an equatorial position of a square-pyramidal site, with Cu–N(azide) = 1.99 Å and a Cu–N–N angle of less than ca. 135°. The cyanide group is also coordinated in an equatorial position, with Cu–C = 1.97 Å and a Cu–C–N angle of 180°. The multiple-scattering analysis of the linear Cu–C–N group has allowed determination of the C–N distance of the cyano group as 1.18 Å. Unlike azido-SOD, which retains an axial imidazole group at 2.27 Å, the cyano derivative appears to be 4-coordinate, with no evidence for an additional coordinated histidine. Detailed analysis of the outer-shell contributions from the coordinated histidine groups indicates that the imidazole rings are asymmetrically coordinated, with the degree of asymmetry depending on the identity of the derivative. It is suggested that the latter effect results from alteration in N_δ–H-bonding interactions of the coordinated imidazoles with the polypeptide chain.

Interest in the Cu/Zn superoxide dismutase (SOD) stems both from its well-defined coordination chemistry and from the growing importance of its pharmaceutical properties.[2] The enzyme is invoked increasingly as a model for non-blue copper proteins[3] since it exhibits many of the chemical and spectroscopic properties of this class of enzymes, including the ability to bind anions,[2,4,5] but remains the only member for which a high-resolution crystal structure is available.[6] The dismutation of superoxide (eq 1) is

$$2HO_2^{\bullet -} = O_2 + H_2O_2 \qquad (1)$$

catalyzed by the copper atom, which is coordinated to four histidine residues in the oxidized form, one histidine forming a bridge to the neighboring zinc atom. The stereochemistry at both copper and zinc approximates to a flattened tetrahedron. An essential arginine residue (Arg-141)[7] is located in the active-site pocket

(1) (a) Department of Chemistry, University of Manchester Institute of Science and Technology, U.K. (b) S.E.R.C. Daresbury Laboratory, Warrington, Cheshire, U.K.
(2) (a) Valentine, J. S.; Pantoliano, M. W. In *Copper Proteins*; Spiro, T. G., Ed.; Wiley: New York, 1981; pp 291-358. (b) Fee, J. A. In *Metal Ions in Biological Systems*; Sigel, H., Ed.; Marcel Dekker: New York, 1981; Vol. 13, pp 259-298. (c) Fielden, G. M.; Rotilio, G.; In *Copper Proteins and Copper Enzymes*; Lontie, R., Ed.; CRC Press: Boca Raton, FL, 1984; Vol. 2, pp 27-61. (d) Cass, A. E. In *Metalloproteins, Part I: Metal Proteins with Redox Roles*; Harrison, P. M., Ed.; Macmillan: London, 1985; pp 121-156. (e) Steinman, H. M. In *Superoxide Dismutase*; Oberly, L., Ed.; CRC Press: Boca Raton, FL, 1982; Vol. I, pp 11-68. (f) Forty-eight papers on the pharmacological and clinical aspects of superoxide and superoxide dismutase have been published in *Superoxide and Superoxide Dismutase in Chemistry, Biology and Medicine*, Proceedings of the 4th International Conference on Superoxide and Superoxide Dismutase, Rome, 1985; Rotilio, G., Ed.; Elsevier: Amsterdam, 1986; pp 493-681.
(3) Malkin, R.; Malmstrom, B. G. *Adv. Enzymol.* **1970**, *33*, 177-244.
(4) (a) Fee, J. A.; Gaber, B. P. *J. Biol. Chem.* **1972**, *247*, 60-65. (b) Bertini, I.; Borghi, E.; Luchinat, C.; Scozzafava, A. *J. Am. Chem. Soc.* **1981**, *103*, 7779-7783. (c) Dooley, D. M.; McGuirl, M. A. *Inorg. Chem.* **1986**, *25*, 1261-1264.
(5) Blackburn, N. J.; Collison, D.; Sutton, J.; Mabbs, F. E. *Biochem. J.* **1984**, *220*, 447-454. (b) Barker, R.; Boden, N.; Cayley, G.; Charlton, S. C.; Henson, R.; Holmes, M. C.; Kelly, I. D.; Knowles, P. F. *Biochem. J.* **1979**, *177*, 289-302. (c) Dooley, D. M.; Cote, C. E. *Inorg. Chem.* **1985**, *24*, 3996-4000. (d) Giordano, R. S.; Bereman, R. D.; Kosman, D. J.; Ettinger, M. J. *J. Am. Chem. Soc.* **1974**, *96*, 1023-1026.
(6) (a) Tainer, J. A.; Getzoff, E. D.; Beem, K. M.; Richardson, J. S.; Richardson, D. C. *J. Mol. Biol.* **1982**, *160*, 181-217. (b) Tainer, J. A.; Getzoff, E. D.; Richardson, J. S.; Richardson, D. C. *Nature (London)* **1983**, *306*, 284-287.

0002-7863/87/1509-7162$01.50/0

about 5 Å from the copper,[6,8] and the approach to the active-site crevice is lined by positively charged residues (Lys-134, Lys-120). Chemical[9,10] and theoretical[8,11] considerations have led to the proposal that the anionic substrate, O_2^-, is directed along a positive electric field gradient produced by these positively charged residues into the active site, where coordination to the Cu(II) center is assisted by hydrogen bonding to Arg-141.

A feature of the coordination chemistry of SOD is its affinity for small linear anions such as cyanide, azide, and thiocyanate, which coordinate to the Cu(II) center, inhibit enzymatic activity, and effect major changes in the spectroscopy of the copper center.[2,4] The structural similarity of these ligands to the superoxide substrate makes anion binding a valuable method of probing structure–function relationships in the Cu/Zn SOD. Studies using interactive molecular graphics have shown that diatomic anions such as either the O_2^- substrate or the inhibitory CN^- fit nicely into a small pit in the surface which lies between Cu(II) and Arg-141,[6b] and experimental evidence that Arg-141 is involved in the binding of cyanide to Cu(II) has been reported.[10] However, interpretation of a large volume of spectroscopic data, including continuous wave[12] and single-crystal EPR,[13] ENDOR,[14] electron spin echo,[15] NMR,[16] and relaxivity measurements,[17] indicates that anions, and in particular cyanide, reorient the coordination sphere so as to result in binding at an equatorial position of a planar or square-pyramidal copper center.[2b]

X-ray absorption spectroscopy[18] offers an important addition to the armory of spectroscopic techniques which have been applied to SOD. We have used EXAFS to provide details of copper–histidine bond lengths of the native protein at a higher resolution than currently available from X-ray crystallography and have confirmed previous proposals for a 3-coordinate Cu(I) site in the dithionite-reduced enzyme.[19]

Recent advances in EXAFS analysis techniques,[20] namely the incorporation of the multiple-scattering interactions which take place between the atoms of aromatic ring systems, have enabled us to simulate the complete, unfiltered, experimental EXAFS spectrum of a number of crystallographically characterized inorganic complexes containing imidazole[21a] or pyridine[21b] such that all the ring atoms are located at their correct positions. Multiple-scattering interactions between three atoms, M–X–Y, are dependent on the M–X–Y angle and attenuate rapidly as this angle decreases from 180°.[23] Multiple scattering will therefore make a major contribution to the EXAFS of anions (such as CN^-) coordinated in a linear fashion to copper and can provide geometric information on the mode of binding. In this paper, we apply a multiple-scattering analysis to the EXAFS of native SOD and its derivatives with cyanide and azide. The results have allowed the geometry of anion coordination to be determined with some confidence and have indicated the nature of other structural changes that accompany anion binding.

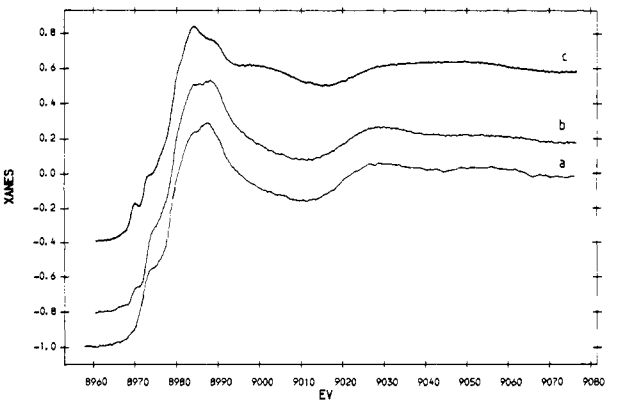

Figure 1. Cu K absorption edges for derivatives of Cu/Zn superoxide dismutase: (a) native enzyme; (b) azide-bound form; (c) cyanide-bound form.

Materials and Methods

Bovine erythrocyte superoxide dismutase was prepared and assayed according to the method of McCord and Fridovich.[24] The final purification step of this procedure involves use of a phosphate salt gradient (2.5–200 mmol dm^{-3}), and many of the spectroscopic studies reported previously have employed phosphate as buffer ion. However, Valentine and co-workers have demonstrated that phosphate inhibits SOD via electrostatic interaction with Arg-141.[10] Thus, although the EPR spectrum of the copper center is unaffected by phosphate binding, the ^{31}P NMR resonance undergoes paramagnetic broadening on account of the proximity of Cu^{2+}. In order to avoid possible complications in the EXAFS analysis of the native enzyme due to long-range scattering from the phosphate group, other buffer systems were examined. PIPES buffer (10–50 mmol dm^{-3}, pH 7.5) was found to induce some precipitation of the protein and was therefore ruled out. Borate buffer (10–50 mmol dm^{-3}) gave EPR parameters of the native enzyme which were identical with those in either phosphate or deionized water over the pH range 6–11, indicating that BO_3^{3-} does not bind to the Cu(II) ion. Binding of borate to Arg-141 was investigated by ^{11}B NMR using a Bruker WP80 spectrometer operating at 25 MHz. The ^{11}B resonance of a 50 mmol dm^{-3} aqueous solution (containing 10% D_2O) of sodium borate, pH 10.2, was measured on its own and in the presence of (i) 18 mg cm^{-3} apo-SOD and (ii) 18 mg cm^{-3} native enzyme. All three samples gave identical NMR spectra (singlet, 45 ppm downfield from $^{11}BH_4^-$), with identical half-line width of 18 Hz. These data indicate that the borate resonance is unaffected by the presence of a Cu^{2+} ion and therefore is not bound in close

(7) (a) Malinowski, D. P.; Fridovich, I. *Biochemistry* **1979**, *18*, 5909–5917. (b) Borders, C. L.; Saunders, J. E.; Blech, D. M.; Fridovich, I. *Biochem. J.* **1985**, *230*, 771–776.

(8) Getzoff, E. D.; Tainer, J. A.; Weiner, P. K.; Kollman, P. A.; Richardson, J. S.; Richardson, D. C. *Nature (London)* **1983**, *306*, 287–290.

(9) (a) Cudd, A.; Fridovich, I. *J. Biol. Chem.* **1982**, *257*, 11443–11447. (b) Marmocchi, F.; Mavelli, I.; Rigo, A.; Stevanato, R.; Bossa, F.; Rotilio, G. *Biochemistry* **1982**, *21*, 2853–2856. (c) Cocco, D.; Rossi, L.; Barra, D.; Bossa, F.; Rotilio, G. *FEBS Lett.* **1982**, *150*, 303–306.

(10) (a) Bermingham-McDonogh, O.; De Freitas, D. M.; Kumamoto, A.; Saunders, J. E.; Blech, D. M.; Borders, C. L., Jr.; Valentine, J. S. *Biochem. Biophys. Res. Commun.* **1982**, *108*, 1376–1382. (b) Mota de Freitas, D.; Valentine, J. S. *Biochemistry* **1984**, *23*, 2079–2082. (c) Mota de Freitas, D.; Valentine, J. S. In *Superoxide and Superoxide Dismutase in Chemistry, Biology and Medicine*, Proceedings of the 4th International Conference on Superoxide and Superoxide Dismutase, Rome, 1985; Rotilio, G., Ed.; Elsevier: Amsterdam, 1986; pp 149–154.

(11) (a) Osman, R.; Bach, H. *J. Am. Chem. Soc.* **1984**, *106*, 5710–5714. (b) Rossi, M.; Sgamellotti, A.; Tarantelli, F.; Bertini, I.; Luchinat, C. *Inorg. Chem.* **1986**, *25*, 1005–1008.

(12) (a) Rotilio, G.; Morpurgo, L.; Giovagnoli, C.; Calabrese, L.; Mondovi, B. *Biochemistry* **1972**, *11*, 2187–2192. (b) Beem, K. M.; Richardson, D. C.; Rajagopalan, K. V. *Biochemistry* **1977**, *9*, 1930–1936.

(13) Lieberman, R. A.; Sands, R. H.; Fee, J. A. *J. Biol. Chem.* **1982**, *257*, 336–344.

(14) Van Kamp, H. L.; Sands, R. H.; Fee, J. A. *Biochim. Biophys. Acta* **1982**, *704*, 75–89.

(15) Fee, J. A.; Peisach, J.; Mimms, W. B. *J. Biol. Chem.* **1981**, *256*, 1910–1914.

(16) Bertini, I.; Lanini, G.; Luchinat, C.; Messori, R.; Monnanni, R.; Scozzafava, A. *J. Am. Chem. Soc.* **1985**, *107*, 4391–4396.

(17) Boden, N.; Holmes, M. C.; Knowles, P. F. *Biochem. J.* **1979**, *177*, 303–309.

(18) (a) Teo, B. K. In *EXAFS Spectroscopy: Techniques and Applications*; Teo, B. K., Joy, D. C., Eds.; Plenum: New York, 1981; pp 13–58. (b) Cramer, S. P.; Hodgson, K. O. *Prog. Inorg. Chem.* **1979**, *25*, 1–39. (c) Garner, C. D.; Helliwell, J. R. *Chem. Br.* **1986**, *22*, 835–840.

(19) (a) Blackburn, N. J.; Hasnain, S. S.; Diakun, G. P.; Knowles, P. F.; Binsted, N.; Garner, C. D. *Biochem. J.* **1983**, *213*, 765–768. (b) Blackburn, N. J.; Hasnain, S. S.; Binsted, N.; Diakun, G. P.; Garner, C. D.; Knowles, P. F. *Biochem. J.* **1984**, *219*, 985–990. (c) Blackburn, N. J.; Hasnain, S. S. In *Biological and Inorganic Copper Chemistry*; Karlin, K. D., Zubieta, J., Eds.; Adenine: Guilderland, NY, 1986; Vol. II, pp 33–42.

(20) (a) Gurman, S. J.; Binsted, N.; Ross, I. *J. Phys. C, Solid State Phys.* **1984**, *17*, 143–151. (b) Gurman, S. J.; Binsted, N.; Ross, I. *J. Phys. C, Solid State Phys.* **1986**, *19*, 1845–1861. (c) Lee, P. A.; Pendry, J. B. *Phys. Rev. B* **1975**, *11*, 2795–2811.

(21) (a) Strange, R. W.; Blackburn, N. J.; Knowles, P. F.; Hasnain, S. S. *J. Am. Chem. Soc.*, preceding paper in this issue. (b) Blackburn, N. J.; Strange, R. W.; Karlin, K. D.; Farooq, A., to be submitted to *J. Am. Chem. Soc.*

(22) (a) McFadden, D. L.; McPhail, A. T.; Garner, C. D.; Mabbs, F. E. *J. Chem. Soc., Dalton Trans.* **1976**, 47–52. (b) Karlin, K. D.; Hayes, J. C.; Hutchinson, J. P.; Hyde, J. R.; Zubieta, J. *Inorg. Chim. Acta* **1982**, *64*, L219.

(23) The angular dependence of the forward scattering and the contribution of multiple scattering to the total EXAFS is summarized in eq 2.1 and 3.1 of ref 20c. The forward scattering, which is energy dependent, peaks strongly at angles of $n\pi$, n = 0, 1, 2, ..., as shown in Figure 5 of ref 20 c.

(24) McCord, J. M.; Fridovich, I. *J. Biol. Chem.* **1969**, *244*, 6049–6055.

proximity to the copper site. Accordingly, EXAFS measurements on native enzyme were carried out in 50 mmol dm^{-3} sodium borate, pH 10.2.

Anion derivatives were prepared as follows. To a 10 mmol dm^{-3} solution of native enzyme was added an amount of chelex-treated sodium azide or potassium cyanide so as to result in a final concentration of anionic ligand of 100 and 60 mmol dm^{-3} of azide and cyanide, respectively. EPR spectra of the derivatives were examined at 9 GHz and found to be identical with literature spectra.[1,4,12]

Samples were loaded into aluminum cells with rectangular apertures (12 × 3 mm) and a sample thickness of 2 mm. EXAFS measurements were carried out in the fluorescent mode[25] on stations 7.1, 8.2, and 9.2 at the SRS, Daresbury Laboratory, under operating conditions of 2.00 GeV and maximum currents of 300 mA. For the native and cyanide samples, the temperature was maintained at 65–75 K using an Oxford Instruments continuous-flow helium cryostat, specially designed for the EXAFS experiments. The temperature of measurement of the azide derivative was 150–130 K. The cyano derivative was measured on station 9.2 using a Si double-crystal order-sorting monochromator whereas the native and azide samples were measured on station 7.1 with a Si 111 monochromator. Harmonic rejection was typically chosen to be 50%. In each case, the monochromator was calibrated in energy space by setting the maximum of the first feature on the absorption edge of metallic copper foil to 8982 eV, measured under conditions identical with those used for the samples.

Nine, six, and four scans were collected and averaged for the native, azide, and cyanide samples, respectively. After conversion of monochromator position to energy and normalization of the edge height, background subtraction was achieved by fitting the smoothly varying part of the absorption to polynomials below and above the absorption edge and subtracting from the experimental absorption spectrum. The background-subtracted, raw EXAFS thus obtained was converted into k space and weighted, usually by k^3, in order to compensate for the diminishing amplitude at high k due to decay of the photoelectron wave. Analysis of the EXAFS was carried out with the program EXCURVE[20] as previously described in detail.[19–23]

Results and Discussion

Absorption Edges. The absorption edge and XANES region (8950–9080 eV) of the X-ray absorption spectra of native, azido, and cyano superoxide dismutase are shown in Figure 1. The native and azido edges are very similar and exhibit a number of poorly resolved shoulders at similar energies. The edge of the cyano derivative, on the other hand, is richer in structure and exhibits a number of sharp features at different energies. Recent simulations of the XANES of the native SOD[26] have indicated that the edge features may arise in part from inter-ring scattering interactions and are very dependent on imidazole ring orientational disorder. Comparison of edge features of the anion derivatives with those of native enzyme would thus suggest that the detailed geometry around Cu(II) in the azido derivative does not differ substantially from that in the native enzyme, whereas some major structural reorientation has occurred as the result of CN^- binding.

These general conclusions are reinforced by comparing the EXAFS of the native enzyme and the two derivatives, shown in Figure 2 with k^2 weighting. The EXAFS of the native enzyme and the azido derivative is qualitatively and quantitatively similar in the range k = 3.5–13, whereas substantial differences are clearly discernible in the spectrum of the cyano derivative.

Multiple-Scattering Approach to EXAFS Analysis. Advances in the techniques of EXAFS analysis pioneered at the Daresbury Laboratory[20,21] have enabled the raw unfiltered EXAFS data to be accurately simulated, and the observed differences in the spectra of the enzyme derivatives can thus be interpreted structurally with some confidence. This involves the incorporation into the calculations of all double- and triple-scattering interactions which occur among the atoms of the imidazole ring system. The multiple-scattering pathways which we have considered are shown in Table I, along with the atom-labeling scheme used for the imidazole ring atoms. Multiple scattering is considered to occur between a minimum of three atoms, for example Cu–N1–C3 in Table I, and makes the maximum contribution when the three

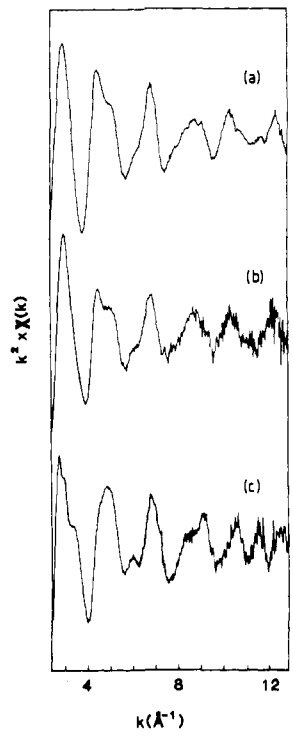

Figure 2. Comparison of the Cu K EXAFS of derivatives of Cu/Zn superoxide dismutase plotted with k^2 weighting: (a) native enzyme; (b) azide-bound form; (c) cyanide-bound form.

Table I. Atom-Labeling Scheme for Imidazole Groups, Pathways, and Expected Angles for Double- and Triple-Scattering Interactions in SOD–Anion Complexes

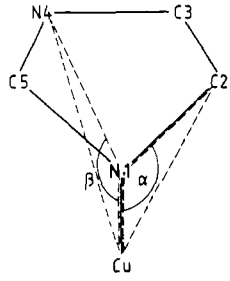

pathway	angle, deg	ref
Cu–N1–C2	+125	38b
Cu–N1–C5	−125	38b
Cu–N1–C3	+163	38b
Cu–N1–N4	−163	38b
Cu–C–N(cyanide)	+180	36, 37, 40–42
Cu–N–N(azide)	+105–145	30–33

atoms are collinear, attenuating rapidly as the M–X–Y angle decreases from 180°.[23] The angle between these three-atom units thus becomes a parameter which must be refined in the fit, so that some limited information concerning imidazole ring orientation can be obtained. The contribution to the EXAFS from the multiple scattering which occurs within these multiatom units is summed and added to the single-scattering contribution to produce the final calculated EXAFS spectrum as described in detail in ref 21a. This procedure necessitates refining Cu–C2 and Cu–C5 interactions separately, and the results have suggested (vide infra) that for the enzyme derivatives the Cu–C2 and Cu–C5 distances are not necessarily equivalent but may split as the result of skewed ring orientation. In the case of the cyano derivative, additional strong multiple scattering is expected from the potentially collinear Cu–C–N group. We therefore have also to consider a multiple-scattering unit composed of the latter three atoms and have been able to refine the Cu–C–N angle. Again, the multiple-scattering method requires the cyano group to be simulated as

(25) Hasnain, S. S.; Quinn, P. D.; Diakun, G. P.; Wardell, E. M.; Garner, C. D. *J. Phys. E: Sci. Instrum.* **1984**, *17*, 40–43.
(26) Alagna, L.; Strange, R. W.; Durham, P.; Hasnain, S. S., to be published.

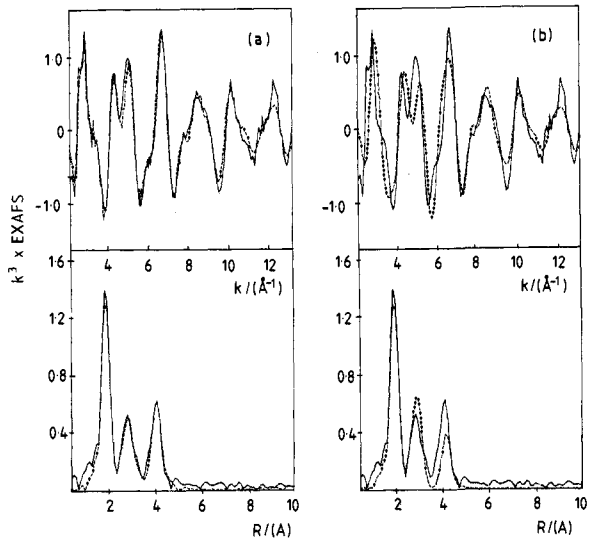

Figure 3. Experimental (solid line) and theoretical (dashed line) k^3-weighted Cu K edge EXAFS and Fourier transform of powdered crystalline tetrakis(imidazole)copper(II) nitrate: (a) simulated with the multiple-scattering method; (b) simulated with single-scattering theory only.

a distinct unit and thus allows the determination of the structural parameters of the cyano group independently from those of coordinated imidazole. However, we have been concerned that distances (obtained as the result of the shells consequently being free to split in the refinement) may be highly correlated, and therefore we have attempted to test the significance of the results by examining the fit index as a function of the magnitude of the splitting.

Reference to the crystal structures of a variety of Cu–imidazole complexes[22a,38] has indicated that the internal imidazole ring geometry is to a good approximation invariant (Table I) such that the radial distances of the second- and third-shell atoms of the ring (i.e., Cu–C2/C5 and Cu–C3/N4) depend only on the Cu–N1 distance, and the angles α and β in Table I.[21] Our cycles of data analysis therefore proceeded as follows. The Cu–N1 distance was first estimated from either the Fourier transform or simulation of the Fourier-filtered first-shell EXAFS. This distance was used to calculate the expected positions of C2/C5 and C3/N4 atoms, assuming fixed ring geometry. The multiple-scattering contribution for this configuration was then calculated by the method described in ref 20 and 21a. Least-squares refinement of the data was then carried out by using the single-scattering approximation to iterate each shell of atoms and their Debye–Waller factors and adding on the multiple-scattering contribution at each stage of the refinement, until a minimum was obtained in the value of the fit index[27] and the best visual fit was obtained between experiment and theory for both EXAFS and Fourier transform. If the iteration procedure produced any significant differences in the distances, the multiple-scattering contribution was recalculated by using the new distances, and a further cycle of refinement was carried out. This procedure was repeated until self-consistency was achieved.

The above procedure was tested on relevant model compounds of known structure containing either imidazole or pyridine coordination. Figure 3a shows a comparison of the experimental and calculated EXAFS and Fourier transform for tetrakis(imidazole)copper(II) nitrate[22a] using the multiple-scattering method. The distances derived from this analysis are compared with crystallographic values in Table II. Agreement is excellent for all atoms of the rings. Figure 3b shows the result of simulating the EXAFS with crystallographic distances but without inclusion of the multiple-scattering contribution. This fit is clearly inadequate. If the fit is allowed to float freely, using only the single-scattering treatment, the least-squares refinement minimizes at values of the distances given in Table II for single-scattering refinement which are clearly in error, as has been reported previously.[19a,21a] Application of a similar analysis to (tris(2-pyridin-2-ylethyl)amine)copper(I) tetraphenylborate ([Cu(TEPA)]$^+$)[22b] gives equally satisfactory agreement between EXAFS and crystallography, as shown in Figure 4 and Table II.

(27) The least-squares fitting (FI) is defined as the weighted sum of the squares of experimental minus theoretical data points: $FI = \sum_i (X(i)_{expt} - X(i)_{theory})^2/N$, where N is the number of data points in the experimental spectrum.

Table II. Parameters Used To Simulate the Cu K EXAFS of Tetrakis(imidazole)copper(II) Nitrate and [Cu(TEPA)][BPh_4] Using the Multiple-Scattering Method[a]

		EXAFS			
	crystal structure	single scattering		multiple scattering	
shell	R_{av}/Å	R/Å	$2\sigma^2$/Å^2	R/Å	$2\sigma^2$/Å^2
	Tetrakis(imidazole)copper(II) nitrate[22a]				
4 N	2.00	2.00	0.005	2.00	0.005
4 C	2.98	2.92	0.010	2.92	0.007
4 C	3.04	3.02	0.010	3.02	0.007
4 C	4.14	3.78	0.010	4.15	0.010
4 C	4.18	3.87	0.010	4.22	0.010
	[Cu(TEPA)][BPh_4][22b]				
3 N(py)	2.018			1.99	0.007
1 N(amino)	2.192			2.18 (8)	0.030
3 C(py)	2.922			2.88	0.007
3 C(py)	2.951			2.94	0.007
3 C(py)	4.241			4.22	0.013
3 C(py)	4.272			4.30	0.013
3 C(py)	4.785			4.71	0.013

[a] The Debye–Waller term ($2\sigma^2$) represents the root-mean-square relative displacement along the direction of the absorber–scatterer vector. The column labeled "single scattering" represents the values of the distances obtained when the data were refined with single-scattering theory only.

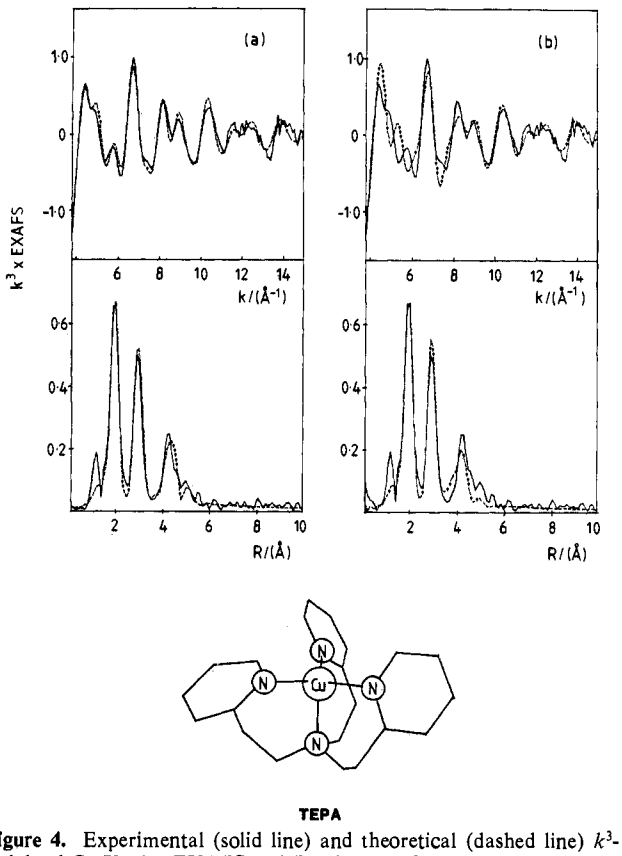

Figure 4. Experimental (solid line) and theoretical (dashed line) k^3-weighted Cu K edge EXAFS and Fourier transform of powdered crystalline [Cu(TEPA)][BPh_4]: (a) simulated with the multiple-scattering method; (b) simulated with single-scattering theory only.

Table III. First-Shell Information: Distances and Debye–Waller Factors for the Groups Coordinated in the Inner Coordination Sphere of Native Superoxide Dismutase and Its Anion Derivatives As Determined by Simulation of the Cu K Edge EXAFS[a]

no. of atoms or groups	distance R/Å	Debye–Waller $2\sigma^2$/Å^2
	Native	
4 imidazoles	2.00	0.008
1 O (water)	2.25	0.006
	Azide	
3 imidazoles	1.99	0.004
1 N (azide)	1.99	0.004
1 imidazole	2.27	0.010
	Cyanide	
3 imidazoles	1.95	0.005
1 C (cyanide)[b]	1.97	0.003

[a] The error associated with the bond lengths is ±0.03 Å. The Debye–Waller term ($2\sigma^2$) represents the root-mean-square relative displacement along the direction of the absorber–scatterer vector. [b] Cu–C–N angle = 180°.

A realistic estimation of errors can be obtained from examination of the agreement between EXAFS-derived distances and the crystallographic values for the model compounds. Thus first-shell (Cu–N1) distances are estimated as ±0.03 Å, second-shell (Cu–C2/C5) distances, ±0.05 Å, and third-shell (Cu-C3/N4) distances, ±0.07 Å. These limits of error are also expected to be applicable to the enzyme systems.

EXAFS Analysis of SOD Derivatives. The EXAFS of the native enzyme and the two anion derivatives have been simulated by using these techniques. The excellent agreement between EXAFS and crystallography for the model compounds demonstrates that the use of the multiple-scattering method makes it possible to locate all the atoms of the imidazole (and pyridine) rings at their correct positions within the above limits of error, such that the internal ring geometry is preserved and the imidazole or pyridine ligands behave as structural units with well-defined geometry. This result is most important, because it implies that the outer-shell positions of imidazole rings in the unknown protein systems can be constrained to take up positions close to those expected for fixed ring geometry, and least-squares minimization restricted to small variations (ca. <0.15 Å) about these initial values. This procedure minimizes the risk of convergence to false local minima and effectively reduces the number of truly independent variables to the first-shell distance, the Debye–Waller factors, and the two angles which define the multiple-scattering pathways (Table I). This allows us to describe the structure of the SOD derivatives in terms of numbers of imidazole groups and their distances from the central copper atom, together with information on the coordinated anionic ligand.

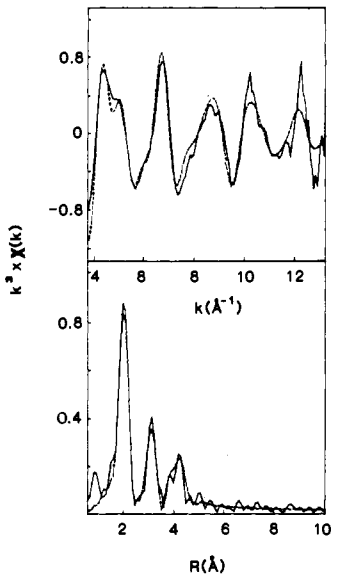

Figure 5. Simulation of the k^3-weighted Cu K EXAFS and Fourier transform of native SOD, using the multiple-scattering method.

Native Enzyme. The EXAFS of the native enzyme can be accurately reproduced with four imidazole groups at an average distance of 1.99 Å and an oxygen atom from solvent at 2.25 Å. The complete fit of theory to experiment for both EXAFS and Fourier transform is shown in Figure 5, and the derived structural parameters for the inner coordination sphere are given in Table III. These first-shell parameters are identical within experimental error with those obtained previously with single-scattering theory.[19b] However, examination of the outer-shell contributions, which are given in Table IV, shows that the multiple-scattering approach locates these at the expected distances for outer-shell C3 and N4 atoms of the imidazole rings, rather than at the shorter distances of ca. 3.8 Å found previously.

The precision with which the position of the solvent oxygen is determined by the EXAFS analysis has been assessed by calculating the value of the least-squares fit index[27] as the Cu–O

Table IV. Imidazole Outer-Shell Geometry: Splitting of C2/C5 and C3/N4 Distances and Cu–N1–C2/C5 and Cu–N1–C3/N4 Angles As Determined by the Multiple-Scattering Analysis and the Improvement in the Least-Squares Fitting Index Which Results upon Splitting of the Shells

		fit index[a]				
	R/Å	split	unsplit	ΔR/Å	$\angle_{obsd}$/deg	$\angle_{calcd}$/deg
			Native			
C2/C5	2.90	2.41	5.11	0.13	115	118[b]
	3.03				−126	−128
C3/N4	4.09			0.17	158	
	4.26				−171	
			Azide			
C2/C5	2.88	7.97	9.62	0.10	120	117
	2.98				−120	−125
C3/N4	4.09			0.10	163	
	4.19				−163	
			Cyanide			
C2/C5	2.94	2.75	8.38	0.25	115	123
	3.19				−129	−147
C3/N4	4.09			0.18	158	
	4.27				−175	

[a] Reference 27. These values may be compared with the values of the fit index for split and unsplit shells of 2.34 and 3.21 Å for tetrabis(imidazole)copper(II) nitrate and 0.83 and 1.14 Å for [Cu(TEPA)][BPh_4], respectively. [b] The calculation of these angles has assumed a constant imidazole N1–C2/C5 of 1.35 Å. In reality, these distances can vary between 1.30 and 1.40 Å, depending on the identity of the imidazole complex, constraints of crystal packing, etc. Thus while agreement is satisfactory for the native enzyme and the azido derivative, it is not so good for the cyano derivative. If, for example, an imidazole N1–C2/C5 distance of 1.40 Å is used, the values for the latter drop to 120 and 141°, which are in better agreement with experiment.

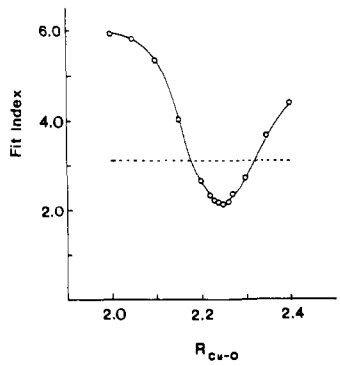

Figure 6. Variation of the k^3-weighted least-squares fit index (defined in ref 27) for native SOD simulations plotted as a function of the first-shell Cu–O distance. The dotted line is the value of the fit index when the first-shell O atom is omitted from the fit.

distance is allowed to vary between 2.00 and 2.40 Å. The results of this analysis are shown in Figure 6. It can be seen that the refinement does indeed lead to a minimum, which is 30% lower than the value of the least-squares fit index obtained with no oxygen present. The value of Cu–O = 2.25 Å corresponding to this minimum is consistent with the distances found for axial type water molecules in a number of square-pyramidal 5-coordinate copper complexes,[28] which typically exhibit Cu–OH distances of around 2.3 Å. However, the X-ray crystal structure[6] suggests that the four imidazole groups in SOD take up a flattened tetrahedral arrangement around the copper, with the solvent molecule occupying a position on the open side of the metal, and this stereochemistry is supported by the highly rhombic EPR spectrum.[12] Thus, although the EXAFS result of an average of four equidistant imidazoles and a longer solvent molecule may suggest square-pyramidal coordination, the site must clearly be considered to be distorted from this ideal stereochemistry. An example of a long equatorial water molecule (Cu–O = 2.225 Å) in a trigonal-bipyramidal $CuS_2N_2(H_2O)$ macrocyclic complex has recently been reported.[29]

Azide Derivative. It can be seen from Figures 1 and 2 that both the XANES and EXAFS of azido-SOD are extremely similar to the XANES and EXAFS of the native enzyme. On the other hand, there is strong evidence in the literature that the azide group coordinates to Cu(II), derived principally from characteristic charge transfer at 378 nm[4a,c] and NMR and EPR spectroscopies.[4a,12] Two coordination modes for azide may be envisaged: (a) substitution of the coordinated water molecule to give a pseudo-square-pyramidal site, with azide occupying an axial position; (b) binding of azide at an equatorial position, accompanied by displacement of a coordinated imidazole to an axial type position. These possibilities have been investigated in our EXAFS analysis shown in parts a and b of Figure 7, respectively. The calculations include multiple scattering from the imidazole rings as well as from the Cu–N–N unit of the coordinated azide. (The Cu–N–N angle is refined as one parameter in the fit.) The simulation shown in Figure 7a has employed four imidazole groups at 2.00 Å and an azide group at 2.23 Å: Figure 7b employs three imidazole groups at 2.00 Å, an azide group at 2.00 Å, and a fourth imidazole at 2.27 Å. Both simulations are good representations of the data. In Figure 7a, the shoulder on the high-R side of the second transform peak is simulated by the multiple scattering from the second nitrogen atom of the azide group at 3.4 Å, with a Cu–N–N angle of 160°. However, trigonometric calculations show that such an arrangement is inconsistent with a Cu–N bond length of 2.23 Å. In Figure 7b, this shoulder is simulated by the C2 and C5 carbon atoms of the longer imidazole group (Cu–imid

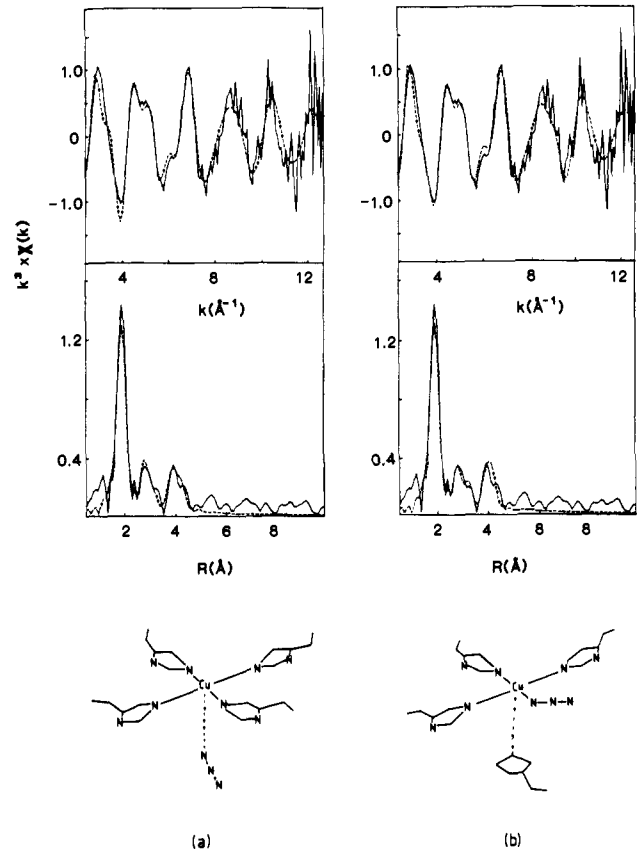

Figure 7. Simulation of the k^3-weighted Cu K EXAFS and Fourier transform of the azido derivative of SOD for two different models using the multiple-scattering treatment: (a) 5-coordinate with an axial azide at 2.23 Å and Cu–N–N = 160°; (b) 5-coordinate with an equatorial azide at 1.99 Å and no multiple scattering from the azide group. See the text for further details.

= 2.27 Å). Furthermore, it is now no longer necessary to include multiple scattering from the Cu–N–N unit of coordinated imidazole, which would imply that the Cu–N–N angle is less than ca. 130°.

Three modes of coordination of azide to copper are found in the literature: terminal, 1,1-bridged, and 1,3-bridged. In no case do Cu–N–N angles exceed 145°. Terminally coordinated azido groups generally exhibit Cu–N–N angles close to 130°.[30] Similar angles are found in 1,1-bridged binuclear complexes.[31] 1,3-Bridged binuclear species generally exhibit smaller Cu–N–N angles, and examples in the range 106–136° are known.[32] Drew and co-workers[33] have reported a 1,3-azido-bridged macrocyclic copper complex with Cu–N1–N2 and Cu–N3–N2 angles of 114 and 143°, but the larger angle of 143° reflects weaker binding of the N3 end of the azide group to the second copper atom. Thus, if the azide group in SOD is coordinated in a terminal fashion, an angle close to 130° would be expected, whereas by analogy to the 1,3-bridged systems, association of the N3 end with Arg-141 would be expected to decrease the Cu–N1–N2 angle.

Our EXAFS analysis therefore supports the model involving equatorial azide binding accompanied by displacement of imid-

(28) (a) Fallon, G. D.; Murray, K. S.; Spethman, B.; Yandell, J. K. Hodgkin, J. H.; Loft, B. C. *J. Chem. Soc., Chem. Commun.* **1984**, 1561–1563. (b) Karlin, K. D.; Gultneh, Y.; Hayes, J. C.; Zubieta, J. *Inorg. Chem.* **1984**, *23*, 521–523.

(29) Addison, A. W.; Rao, T. N.; Reedikj, J.; Van Rijn, J.; Verschoor, G. C. *J. Chem. Soc., Dalton Trans.* **1984**, 1349–1356.

(30) (a) Camarmond, J.; Plumere, P.; Lehn, J.-M.; Agnus, Y.; Louis, R.; Weiss, R.; Kahn, O.; Morgenstein-Badarau, I. *J. Am. Chem. Soc.* **1982**, *104*, 6330–6340. (b) Klaehn, D. D.; Paulus, H.; Grewe, R.; Elias, H. *Inorg. Chem.* **1984**, *23*, 483–490.

(31) (a) Khan, O.; Sikorav, S.; Gouteron, J.; Jeannin, S.; Jeannin, Y. *Inorg. Chem.* **1983**, *22*, 2877–2883. (b) Karlin, K. D.; Hayes, J.; Hutchinson, J. P.; Zubieta, J. *J. Chem. Soc., Chem. Commun.* **1983**, 376–378.

(32) (a) McKee, V.; Zagulis, M.; Dagdigian, J. V.; Patch, M. V.; Reed, C. A. *J. Am. Chem. Soc.* **1984**, *106*, 4765–4772. (b) Sorrell, T. N.; O'Connor, C. J.; Anderson, O. P.; Reibenspies, J. H. *J. Am. Chem. Soc.* **1985**, *107*, 4199–4206. (c) Agnus, Y.; Louis, R.; Gisselbrecht, J. P.; Wiess, R. *J. Am. Chem. Soc.* **1984**, *106*, 93–102.

(33) Drew, M. G. B.; McCann, M.; Nelson, S. M. *J. Chem. Soc., Chem. Commun.* **1979**, 481–482.

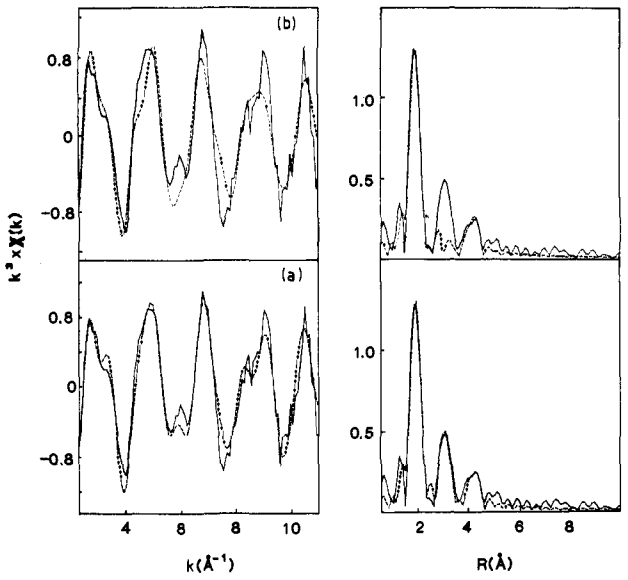

Figure 8. Simulation of the k^3-weighted Cu K EXAFS and Fourier transform of the cyano derivative of SOD using the multiple-scattering treatment: (a) best simulation including the multiple-scattering from the linear Cu–C–N group; (b) effect of omitting the multiple-scattering contribution from the cyano group.

azole to an axial position. This structure has also been proposed on the basis of high-resolution proton NMR studies of azido-Cu/Co SOD reported by Bertini and co-workers.[16] The NMR work has shown that one of the imidazole groups is not influenced by the paramagnetism of the Cu(II) center, which suggests that it is no longer coordinated to copper. Backscattering from neighboring atoms to copper can, of course, arise from nonbonded interactions and does not require the backscatterer to be coordinated. Thus it is possible that the displaced imidazole group is oriented such that the N1 atom is no longer capable of effective hybridization with copper, but may still contribute to the EXAFS spectrum.

It should also be noted the XANES region of both azide and native proteins is very similar, indicating that any structural reorganization at the copper site which occurs as the result of azide binding must be of a rather limited nature. Thus it is probable that, like native enzyme, the copper site of the azido derivative is also distorted from ideal square-pyramidal geometry.[34]

Cyanide Derivative. Simulation of the EXAFS and Fourier transforms of cyano-SOD (Figure 8a) indicates that the considerable spectral changes which are elicited by cyanide binding are the result of a shortening of the Cu–imidazole bond lengths to 1.95 ± 0.03 Å and coordination of CN^- at 1.97 ± 0.03 Å. (It should be noted that the Cu–N(imid) and Cu–C(cyanide) first-shell distances are highly correlated and are probably not separable within the limits of the EXAFS analysis.) The second-shell peak in the transform is much broader than the corresponding peak of either the native enzyme or the azide derivative and can only be simulated satisfactorily if a multiple-scattering contribution from the Cu–C–N (coordinated cyanide) unit is included. (The importance of multiple scattering in fitting the EXAFS is illustrated in Figure 8b in which the MS contribution of the cyanide group has been omitted.) The analysis places the N atom of the cyano group at 3.15 Å from the copper atom, with a Cu–C–N angle of 180°. The cyanide group is thus coordinated in a collinear fashion as expected, and the value of the C–N bond can be calculated to 1.18 Å.

We have attempted to estimate the precision with which the structural parameters of the cyano group are determined using

(34) The suggestion that the azide derivative has axial symmetry is derived principally from the axially symmetric 35-GHz EPR spectrum reported by Rotilio et al. (ref 13a). We have recently observed however that under optimal spectrometer conditions, a rhombic azide spectrum is obtained. The rhombicity of the spectrum is less than that of the native enzyme.

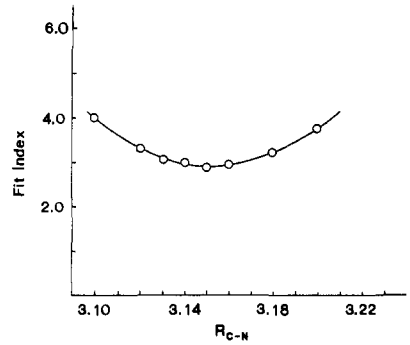

Figure 9. Variation of the k^3-weighted fit index (defined in ref 27) for cyano-SOD simulations as a function of C–N(cyanide) bond length.

a procedure similar to that employed for the solvent oxygen atom. In this case the value of the Cu to N(cyanide) (and thus the value of the C–N(cyanide) bond) has been allowed to vary, and the fit index calculated, while leaving all other parameters constant at their values given in Tables III and IV. In this analysis, it has been necessary to recalculate the multiple-scattering contribution from the cyano group at each of the values of Cu–N chosen.[35] The results, shown in Figure 9, indicate a minimum at 3.15 Å and demonstrate that the parameters for the cyano group are well defined.

The decrease of 0.05 Å in the Cu–imidazole bond length indicates that an increase in ligand field strength has occurred as the result of cyanide binding. This is in line with the blue shift in d–d absorption bands,[4a] the large value of A_{11} (18.8 mT), and the appearance of well-resolved nitrogen superhyperfine structure[4,12-14] in both parallel and perpendicular regions of the X-band EPR spectrum. These and other spectral properties have been interpreted previously in terms of a square-planar structure in which three imidazoles and one cyanide ligand coordinate to the Cu(II) ion.[13,14] This implies that the fourth imidazole has been completely displaced. The present study reinforces this conclusion, since we find no evidence for the presence of an imidazole group at a longer (axial type) position. Any trans influence exerted by the cyano group leading to a shortening of the Cu–N distance trans to the cyano group, as suggested by ENDOR,[14] does not appear to be resolvable by EXAFS (although the larger splitting of outer-shell C2/C5 and C3/N4 atoms observed in the cyano derivative (vide infra) could be related, at least in part, to an unresolved splitting of the first-shell distances).

The structural parameters deduced for coordinated cyanide in SOD have been compared with Cu–C and Cu–N bond lengths of the known crystallographically characterized Cu(II)–cyano complexes[36,37,40-42] in Table V. The values found for SOD are entirely comparable with those of the Cu(II)–CN model complexes. The complex $[Cu_2(tren)_2CN_2](BPh_4)$ in Table V contains a Cu–CN···H–N–Cu interaction which is similar to the H-bond proposed between the CN^- group in SOD and Arg-141. The Cu–C bond length of 1.97 Å and C–N bond length of 1.13 Å are not significantly different from the corresponding distances in the other (non-hydrogen-bonded) cyano complexes, although like cyano-SOD, the Cu–C distance of the tren complex is at the upper

(35) The simulations are more sensitive to the position of the cyanide N atom than the cyanide C atom, since the latter is subsumed under the large first-shell Cu–imidazole peak.

(36) (a) Tyagi, S.; Hathaway, B. J. *J. Chem. Soc., Dalton Trans.* **1983**, 199–203. (b) Anderson, O. P. *Inorg. Chem.* **1975**, *14*, 730–734.

(37) Duggan, M. D.; Jungst, R. G.; Mann, K. R.; Stucky, G. D.; Hendrickson, D. N. *J. Am. Chem. Soc.* **1974**, *96*, 3443–3450.

(38) No splitting of the angular parameters is necessary in the analysis of the imidazole model compounds.

(39) McFadden, D. L.; McPhail, A. T.; Gross, P. M.; Garner, C. D.; Mabbs, F. E. *J. Chem. Soc., Dalton Trans.* **1975**, 263–268.

(40) Anderson, O. P.; Packard, A. B.; Wicholas, M. *Inorg. Chem.* **1976**, *15*, 1613–1618.

(41) Anderson, O. P.; Packard, A. B. *Inorg. Chem.* **1980**, *19*, 2941–2945.

(42) Schlemper, E. O.; Hussain, M. S.; Murmann, R. K. *Acta Crystallogr., Sect. B: Struct. Crystallogr. Cryst. Chem.* **1981**, *37B*, 234–237.

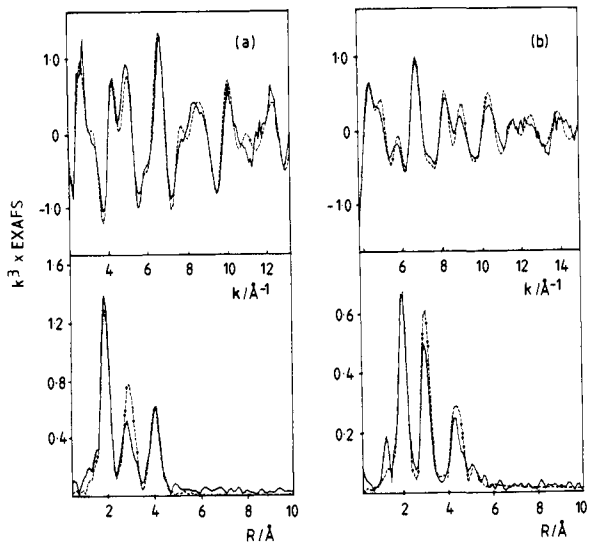

Figure 10. Splitting of outer shells in imidazole and pyridine model compounds. The effect of constraining the outer shells to be unsplit for (a) tetrakis(imidazole)copper(II) nitrate and (b) [Cu(TEPA)][BPh_4].

end of the range for equatorial coordinated CN^-. Thus the parameters of the CN^- group in SOD are certainly not inconsistent with a H-bonded structure. Further examination of the data in Table V also reveals that axial coordination of cyanide in square-pyramidal geometry leads to longer Cu–C distances in excess of 2.04 Å. While any conclusions based on comparisons with the rather limited number of available cyano–Cu(II) structures must be tentative, the data appear to confirm the assertion that cyano-SOD contains equatorially coordinated CN^-.

Comparison of the Structures of the SOD Derivatives. Comparison of the EXAFS analysis for native SOD and its azido and cyano derivatives provides insights into some of the structural changes which accompany anion binding to copper. Table IV lists the second-shell (C2/C5) and third-shell (C3/N4) distances for each of the three enzymes. It can be seen that a splitting of these distances occurs when the multiatom units which define the multiple-scattering pathways are allowed to refine separately, as discussed above. The magnitude of the observed splitting depends on the identity of the enzyme, and satisfactory fits to the data, particularly for the cyanide derivative cannot be obtained which do not include split second and third shells. To document further the significance of the splitting, the values of the fit index with and without split shells is given in Table IV, while Figures 10 and

Table V. Structural Parameters for the Cyano Complex of Cu/Zn SOD Compared with Those of Other Cu(II)–Cyano Complexes[a]

complex	geometry	Cu–C/Å	C–N/Å	Cu–C–N/deg
[Cu(terpy)CN]$^{+}$ [40]	spy eq CN	1.92	1.14	177
[Cu(cyclops)CN] [41]	spy ax CN	2.042	1.14	173.2
[Cu(pnao)CN] [42]	spy ax CN	2.154	1.112	175.6
[Cu_2(tren)$_2CN_2$]$^{2+}$ [37]	tbpy ax CN	1.97	1.13	177
[Cu(phen)$_2$CN]$^{+}$ [36b]	tbpy eq CN	1.935	1.161	177.8
[Cu(bpy)$_2$CN]$^{+}$ [36a]	tbpy eq CN	1.974	1.144	179.0
Cu/Zn SOD-CN		1.97	1.18 (4)	180

[a] Abbreviations: terpy = 2,2′,2″-terpyridyl, cyclops = difluoro(3,3′-(trimethylenedinitrilo)bis(2-butanone oximato))borato, pnao = 3,3′-(1,3-propanediamino)bis(3-methyl-2-butanone oximato), tren = 2,2′,2″-triaminotriethylamine, phen = 1,10-phenanthroline, bpy = 2,2′-bipyridyl, spy = square pyramidal, tbpy = trigonal bipyramidal, eq = equatorial.

11 respectively show the fits to EXAFS and Fourier transforms of the model compounds and enzyme derivatives with second- and third-shell distances constrained to be unsplit. In Figure 12, the value of the fit index has been plotted as a function of the magnitude of the splitting of the second shell for the cyano derivative, with all other parameters kept constant; this analysis indicates that the splitting leads to a true minimum.

For the native and azide-bound enzymes, splittings of 0.13 and 0.10 Å are found for the C2/C5 carbons, respectively. Such splittings are not significantly above the estimated maximum error associated with the second-shell carbon atoms and may in part reflect a spread of copper–imidazole distances. It should be noted in this respect that the Debye–Waller term for the first-shell average Cu–N1 distances of native enzyme is unusually large, suggesting an inequivalence of Cu–N1 distances. Notwithstanding, satisfactory fits to second and third shells cannot be obtained merely by increasing Debye–Waller factors. Also, a much larger splitting of 0.28 Å is found for the Cu–C2/C5 shell of atoms in the cyano derivative. Table IV also gives the values obtained by refining the angles between these ring atoms and the Cu–N1 vector as required by the multiple-scattering analysis. (These angles, together with expected values for symmetrical imidazole coordination, are defined in Table I.) Several pieces of evidence point to distorted imidazole ring coordination as an additional factor contributing to the splitting of the outer shells. (i) No equivalent

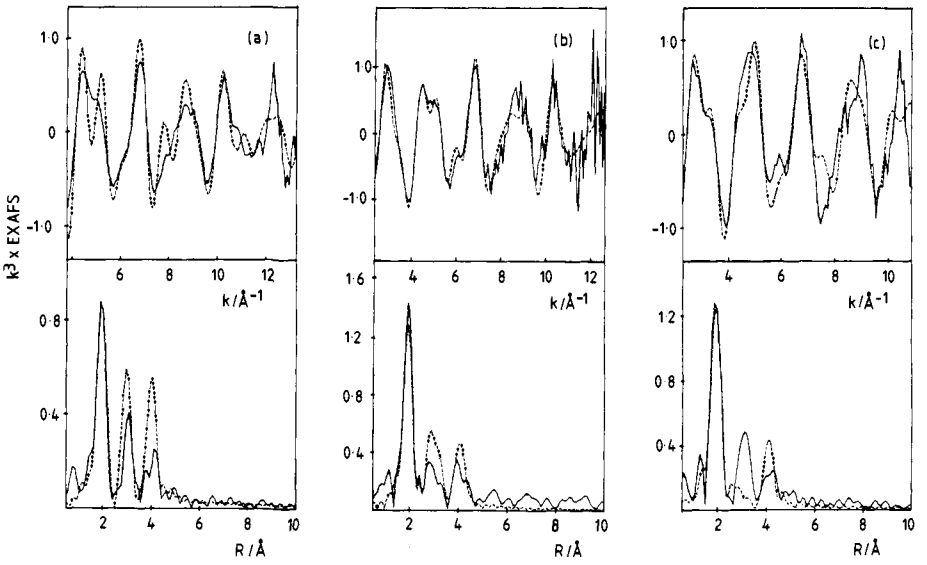

Figure 11. Splitting of outer shells in SOD derivatives. Effect of constraining outer shells to be unsplit in (a) native SOD, (b) azido-SOD, and (c) cyano-SOD.

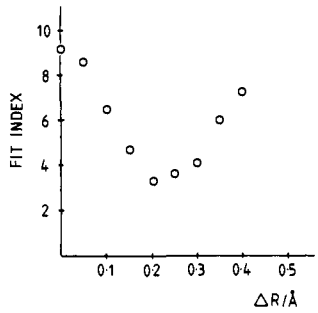

Figure 12. Variation in the k^3-weighted fit index as a function of the splitting of the C2/C5 shell of cyano-SOD.

splitting of the first shell is found; (ii) splittings of similar magnitude to C2/C5 shells are found for the outermost C3/N4 shells (Table IV); (iii) both pairs of angles Cu–N1–C2/C5 and Cu–N1–C3/N4 are themselves split in the native enzyme and the cyano derivative.

The data can be interpreted in terms of a small rotation of the imidazole ring about the normal to the Cu–N1 vector, such that the Cu–C2 distance is no longer equal to the Cu–C5 distance. In Table IV we have also calculated the angular rotation necessary to reproduce the observed splitting of the bond lengths. The correspondence between calculated and experimental values is reasonable. It must be stressed, however, that the analysis can only give the average of any distortion of coordination of individual rings and consequently should be interpreted with caution.

Nevertheless, it is of interest to consider possible structural interpretations. Splitting of C2/C5 and C3/N4 distances of the order of 0.05 Å are observed in the EXAFS analysis of Cu(imid)$_4$(NO$_3$)$_2$ and other imidazole complexes[21a] and does indeed represent the average of the disorder apparent in the corresponding distances in the crystal structures.[21,22,38] The splittings observed in the enzyme case, particularly the cyano derivative, are larger and must arise from a different mechanism. In the case of hexakis(imidazole)copper(II) nitrate, the axial imidazole groups, which are located at 2.6 Å from the copper, hydrogen bond via their protonated N4 atoms to the nitrate counterion, and the optimization of the hydrogen-bonding interaction causes the rings to rotate in the direction of the counterion and introduces an inequivalence of C2 and C5 positions, with Cu–N1–C2 and Cu–N1–C5 angles of 116° and 128°, respectively.[39] The crystal structure of native SOD[6] indicates that the protonated N4 atoms of His-44, His-46, and His-118 hydrogen bond to Asp-122 (carboxyl O), Gly-59 (peptide O), and Gly-139 (peptide O), respectively. The corresponding N atom of His-61 is coordinated to the Zn atom, and examples of substantial inequivalence of the imidazolate C2 and C5 positions of imidazolate-bridged binuclear copper complexes are known (for example C2–N1–Cu = 120.9°, C5–N1–Cu = 132.6°).[43] It is not unreasonable to suppose that hydrogen-bonding interactions, and/or the requirements of zinc coordination, could compete with the copper ion in providing the driving force for imidazole ring orientation. The large distortions from ideal histidine coordination at copper, which are suggested by the cyanide EXAFS data, would then imply that the attainment of regular square-planar geometry at the Cu(II) center can only be achieved at the expense of these secondary (hydrogen) bonding interactions and that the lowest energy configuration represents a compromise involving skewed ring orientation.

Recent ab initio calculations from two groups[11] have independently concluded that the mechanism of dismutation of superoxide involves the prior formation of a Cu(II)–superoxo complex which is stable toward decomposition to Cu(I) and dioxygen until reduced by a second molecule of O_2^-. The results of the present study of cyanide binding, together with the suggestion (derived from computer modeling of substrate docking on the enzyme surface) that superoxide and cyanide may share a common binding site,[8] then raise the interesting possibility that the superoxide bound form could itself represent a strained or entactic state.

Acknowledgment. We gratefully acknowledge financial support from S.E.R.C. (Grant GR/C/94285 to N.J.B. and S.S.H.) and a studentship to L.M.M. We also thank the Daresbury Laboratory for use of facilities. We acknowledge particularly the useful discussions with Dr. Peter Knowles during the course of the study.

Supplementary Material Available: Raw Cu K-edge X-ray absorption data for tetrakis(imidazole)copper(II) nitrate (Table VI), [Cu(TEPA)][BPh$_4$] (Table VII), Cu/Zn superoxide dismutase (Table VIII), azido-SOD (Table IX), and cyano-SOD (Table X) (45 pages). Ordering information is given on any current masthead page.

(43) Coughlin, P. K.; Martin, A. E.; Dewan, J. C.; Watanabe, E.; Bulkowski, J. E.; Lehn, J.-M.; Lippard, S. J. *Inorg. Chem.* **1984**, *23*, 1004–1009.